Photoconductivity in Metal–Organic Framework (MOF) Thin Films

*Xiaojing Liu, Mariana Kozlowska, Timur Okkali, Danny Wagner, Tomohiro Higashino, Gerald Brenner-Weiß, Stefan M. Marschner, Zhihua Fu, Qiang Zhang, Hiroshi Imahori, Stefan Bräse, Wolfgang Wenzel, Christof Wöll, and Lars Heinke**

Abstract: *Photoconductivity is a characteristic property of semi conductors. Herein, we present a photo conducting crystalline metal organic framework (MOF) thin film with an on off photocurrent ratio of two orders of magnitude. These oriented, surface mounted MOF thin films (SURMOFs), contain porphyrin in the framework backbone and C_{60} guests, loaded in the pores using a layer by layer process. By comparison with results obtained for reference MOF structures and based on DFT calculations, we conclude that donor acceptor interactions between the porphyrin of the host MOF and the C_{60} guests give rise to a rapid charge separation. Subsequently, holes and electrons are transported through separate channels formed by porphyrin and by C_{60}, respec tively. The ability to tune the properties and energy levels of the porphyrin and fullerene, along with the controlled organiza tion of donor acceptor pairs in this regular framework offers potential to increase the photoconduction on off ratio.*

Metal organic frameworks (MOFs) are crystalline, nano porous hybrid materials composed of metal nodes connected by organic linker molecules.[1] In recent years, in addition to applications in gas loading and separation,[2] the electrical and electronic properties of MOFs have started to attract substantial attention.[3] In this context, taking advantage of the enormous MOF chemical space, with the number of characterized members of this material's class approaching 100 000,[4] various MOF applications have been investigated, ranging from electrocatalysis[5] over field effect transistor[6] to energy storage.[7] It was found that the conductivity of the MOF material can be significantly increased by loading it with molecules, such as ferrocene,[3c] TCNQ,[3b] or C_{60} fullerene.[8] C_{60} fullerenes are attractive charge acceptors, since the delocalized π systems give rise to a large electron affinity and strong stability.[9] In addition, they show efficient charge separation upon illumination.[10] An interesting band struc ture of C_{60} embedded in the regular MOF pores was theoretically predicted.[11] On the other hand, MOFs with porphyrin linker molecules allow semi conductor light har vesting applications in photovoltaic[12] devices and for photo catalysis.[13] These applications take advantage of the fact that porphyrins are excellent electron donors with delocalized π systems.[14] In the visible region, porphyrins exhibit sharp and intensive absorption bands, ideal for application in light harvesting.[15] To this end, porphyrins are often integrated as active components in various opto electronic devices.[12,16] Furthermore, the porphyrin properties can be tailored by various methods of organic chemistry, for example, by adding electron rich or electron poor groups, allowing to tune photon absorption and other photophysical properties of the mate rial. Combining porphyrin with fullerene results in electron donor acceptor pairs.[17] The light induced electron transfer in such dyads was investigated in solution;[17] and it was demonstrated that materials of such molecules are suitable for applications such as organic solar cells.[18]

Recently, remarkable photoconductance in MOFs incor porating percolated titania nanoparticles has been reported.[19] Irradiation with UV light of 266 nm wavelength (4.66 eV) resulted in a pronounced increase of electron mobility as detected by terahertz spectroscopy. Direct meas urements of the photoinduced changes in the electrical conductivity, however, were not presented, likely due to problems in providing good electrical contacts to MOF powders under light irradiation. Photoconductivity in MOFs with functional organic moieties has not yet been reported, although the virtually unlimited possibilities to tune the properties of such materials are extremely attractive.

For directly measuring the photocurrent, as well as for device applications, for example, in light sensors, the MOF material must be provided in the form of thin films. Thus, we have used surface mounted MOF thin films (SURMOFs)[20] grown on suitably functionalized substrates, providing inter digitated bottom contacts. This approach allows the measure ment of electrical properties of empty and loaded MOFs in a straightforward and reproducible fashion. Herein, several different MOF structures were investigated: While SUR MOFs fabricated from phenyl based linkers did not respond

[*] X. Liu, T. Okkali, Dr. G. Brenner Weiß, Dr. Z. Fu, Q. Zhang, Prof. C. Wöll, Dr. L. Heinke
Institute of Functional Interfaces (IFG)
Karlsruhe Institute of Technology (KIT)
76344 Eggenstein Leopoldshafen (Germany)
E mail: lars.heinke@kit.edu

Dr. M. Kozlowska, Prof. W. Wenzel
Institute of Nanotechnology (INT), KIT
76344 Eggenstein Leopoldshafen (Germany)

D. Wagner, S. M. Marschner, Prof. S. Bräse
Institute of Organic Chemistry (IOC), KIT
76131 Karlsruhe (Germany)

Dr. T. Higashino, Prof. H. Imahori
Department of Molecular Engineering, Graduate School of Engi neering, Kyoto University
Kyoto 615 8510 (Japan)

Prof. S. Bräse
Institute of Toxicology and Genetics (ITG), KIT
76344 Eggenstein Leopoldshafen (Germany)

to light illumination, even after loading with fullerenes, SURMOFs fabricated from different porphyrinic linkers revealed superb photoconducting properties, likely a result of the interesting photophysical properties of these com pounds.[12] While the electrical resistivity of these porphyrinic MOF thin films is found to be rather high, the conductivity increased tremendously when embedding C_{60} molecules in the nanopores of these highly oriented SURMOFs, yielding C_{60}@Zn(TPP) (TPP = 5,15 bis (3,4,5 trimethoxyphenyl) 10,20 bis (4 carboxyphenyl) porphyrinato zinc(II), see Figure 1). Remarkably, these MOF thin films showed pro

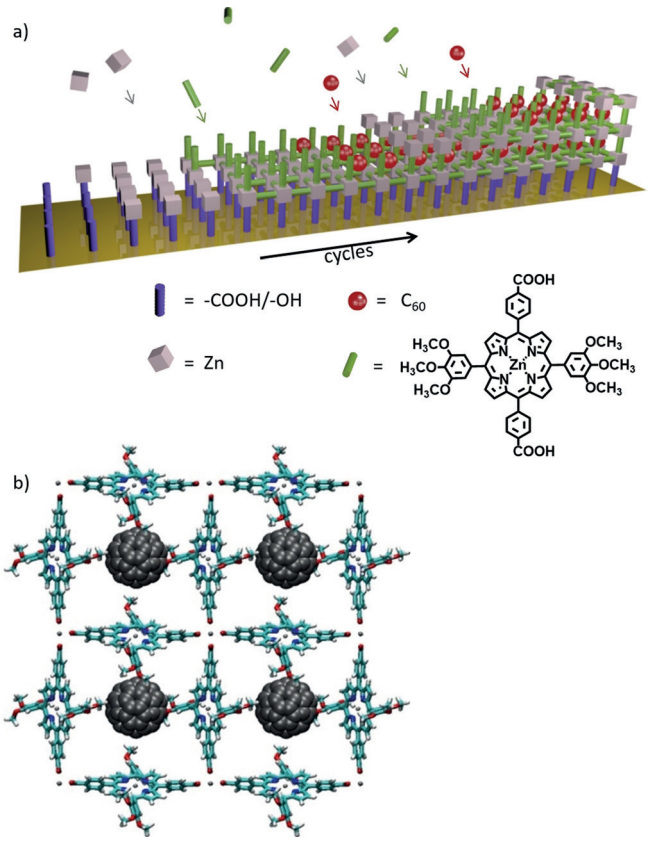

Figure 1. a) Sketch of the layer by layer SURMOF synthesis. The com ponents of C_{60}@Zn(TPP) are shown. b) The structure of C_{60}@Zn(TPP). O red, Zn dark gray, N blue, H white. For clarity, C in MOF scaffold is shown in cyan, C of fullerene is gray.

nounced photoconduction features: the electrical conductiv ity increased by 2 orders of magnitude when irradiated with visible light of 455 nm (2.72 eV). Detailed theoretical inves tigations using density functional theory (DFT) and time dependent DFT calculations revealed the origin of the MOF photoconductivity. First, light is absorbed by the porphyrin moieties. Subsequently, the large electron affinity of the C_{60} results in rapid charge separation.

For the sample preparation, Zn(TPP) and C_{60}@Zn(TPP) SURMOF thin films as well as the phenyl based Cu(BPDC) SURMOF films were synthesized directly on the functional ized electrode in a step by step fashion by alternately spin coating the ethanolic metal acetate solution and the ethanolic linker molecule solution on the substrate, Figure 1 (BPDC = biphenyl dicarboxylate). The C_{60} molecules were loaded in the MOF pores during the synthesis by spin coating the C_{60} solution on the substrate after each linker step, see Figure 1.

The crystallinity of Zn(TPP) and Cu(BPDC) SURMOFs with and without embedded C_{60} was monitored by X ray diffraction (XRD), Figures 2 a, Figures S1 and S6 in the

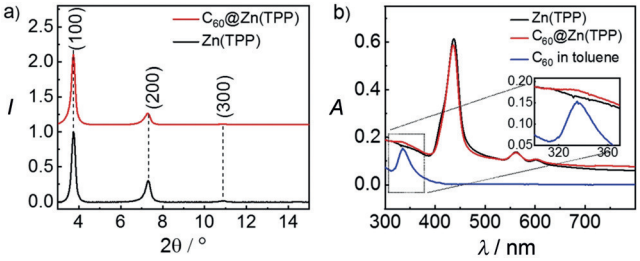

Figure 2. X ray diffractograms (a) and UV/Vis absorption spectra (b) of Zn(TPP) and C_{60}@Zn(TPP) SURMOFs. The UV/Vis spectrum of C_{60} solution in toluene is also shown. The inset shows a magnification from 300 nm to 370 nm.

Supporting Information. The experimental XRD data match well with the calculated diffractogram of the target structure. The absence of the (110), (001), (101), and (111) diffraction peaks reveals a high degree of orientation of the SURMOFs, that is, the films are grown predominantly along the (100) orientation (see Figure S1). The XRD data recorded for C_{60}@Zn(TPP) and Zn(TPP) also reveal that embedding C_{60} did not affect the crystallinity of Zn(TPP), that is, diffraction peak positions did not change and also the peak width was the same as before the loading. Importantly, however, the form factors showed substantial changes. The ratio of the (100) to (200) peak intensities increases from 3.33 for Zn(TPP) to 6.25 for C_{60}@Zn(TPP). This change in form factor is a consequence of the change in electron density, which increased substan tially within the pores by loading them with C_{60}. Note that an exclusive decoration of the outer MOF surface can be excluded from this form factor change; such a change in relative diffraction peak intensities is only possible by affecting virtually every MOF pore.[21]

The UV/Vis absorption spectrum of C_{60}@Zn(TPP) pro vide further evidence of the successful loading with C_{60}, Figure 2 b. The absorption bands at 436 nm, 561 nm, and 600 nm belong to the porphyrin chromophore, whereas the band at 330 nm originates from the C_{60}. From the relative intensity of the UV/Vis absorption bands, the ratio of C_{60} to the porphyrin each unit cell could be determined and was found to be 0.92, indicating that almost every unit cell of the porphyrin MOF contains a C_{60} molecule. For details, see Figure S2. This value was verified by HPLC mass spectrom etry of the dissolved SURMOF sample, which showed an average loading of 0.90 C_{60} molecules per unit cell (Fig ure S3).

The IR spectra of Zn(TPP) and C_{60}@Zn(TPP) are displayed in Figure S4. The bands at approximately 1590 cm^{-1} and 1410 cm^{-1} of both MOFs are assigned to the carboxylate asymmetric and symmetric stretching modes. The

band at 1425 cm^{-1} observed for C_{60}@Zn(TPP) appears after embedding of C_{60}.

To further characterize the as synthesized MOF films, atomic force microscopy (AFM) was carried out to inves tigate the morphology and film thickness. The images in Figure S5c, S5d indicate that the Zn(TPP) and C_{60}@Zn(TPP) are homogenous films with thicknesses of approximately 50 nm. Such MOF films are sufficiently thin, allowing the entire illumination of the sample, as also seen by the UV/Vis spectrum (see Figure 2b) with a maximum absorbance of 0.6 absorption units.

The electrical conductivities of the SURMOF samples deposited on substrates with interdigitated gold electrodes were determined by 2 probe DC conduction measurements. Cu(BPDC) SURMOF 2, a phenyl based MOF structure, showed no significant increase upon irradiation with various wavelengths of the visible spectra (Figure S7a). Cu(BPDC) with empty pores (thickness is 270 nm, see Figure S5a) shows a very low conductivity of approximately 2×10^{-13} $S m^{-1}$ (applied voltage was 2 V). The conductivity of the MOF thin film increased by approximately 4 orders of magnitude upon loading with C_{60}, see Figure S7b. However, the con ductivity is still only slightly affected by light irradiation, for example, the current increases by less than 10% when irradiated with light of 455 nm wavelength.

A rather different photoresponse was observed for the porphyrinic SURMOFs, although the lattice constants and pore sizes of Zn(TPP) SURMOF 2 and Cu(BPDC) SURMOF 2 are very similar, see the XRD data reproduced in Figures S1 and S6. Zn(TPP) SURMOFs, without C_{60} embedment, shows a conductivity of approximately 1.5×10^{-11} $S m^{-1}$ (see Figure S7c), which is low but clearly higher than that of empty Cu(BPDC). In pronounced contrast to the MOF thin films built with the phenyl based linkers, the irradiation with light results in a substantial increase in the conductivity of the porphyrinic SURMOF.

Embedding fullerene in the porphyrin SURMOFs increases the electrical conductivity. When applying 2 V to the C_{60}@Zn(TPP) sample, the current in the dark is approx imately 0.11 nA, corresponding to a conductivity of 1.5×10^{-9} $S m^{-1}$. Irradiation with light substantially increases the current (Figure 3). The observed change in photoconductivity strongly depends on photon wavelength. The largest increase is obtained at 455 nm, that is, by exciting the porphyrin Soret band. There, a value of approximately 9 nA is reached, corresponding to a conductivity increase upon illumination by 2 orders of magnitude.

This observation, and the comparison with the previous reference experiments, indicates that the observed photo conductivity in C_{60}@Zn(TPP) SURMOFs must be related to a cooperative effect of the porphyrin moieties and the C_{60} guests.

The current voltage curve, Figure 3b, shows that, upon illumination, the conductivity of C_{60}@Zn(TPP) increases over the entire voltage range between -5 V and $+5$ V. In the dark, the current increases with voltage more than linearly, roughly exponentially. This is an indication that more conducting paths become available with increasing voltage. Upon irradi ation with light, a different scenario is observed. For light of

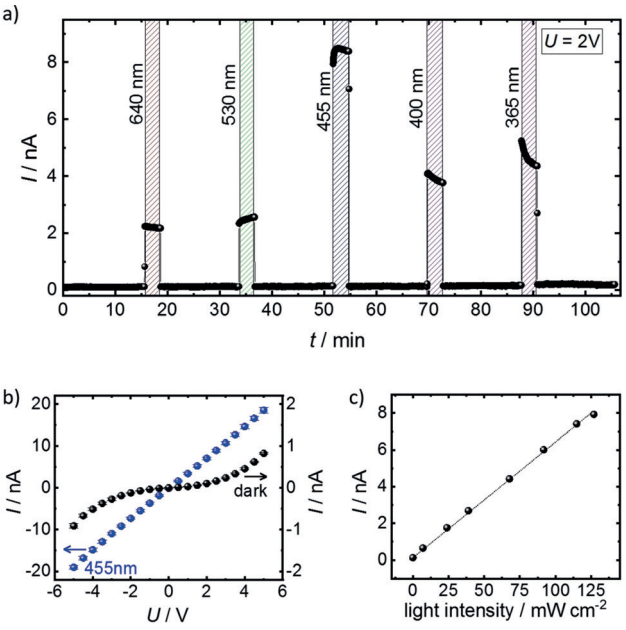

Figure 3. Photoconduction in C_{60}@Zn(TPP). a) The DC current *I* at a voltage of 2 V is measured while the sample is irradiated with light of 640 nm, 530 nm, 455 nm, 400 nm and 365 nm wavelength. The current without light irradiation is 0.11 nA. The photoconduction action spectrum is shown in Figure S11. b) The current voltage curve of the sample in the dark (black spheres) and under irradiation with 455 nm (blue spheres). The log plot of the data is present in Figure S8. c) The photocurrent at different intensities of the 455 nm light irradiation.

455 nm, the photocurrent is proportional to the voltage, revealing almost ideal ohmic conduction behavior with a conductivity of 1.3×10^{-7} $S m^{-1}$. A linear correlation between photocurrent and the intensity of incident light is observed (Figure 3c and Figure S9), demonstrating that two photon processes appear to be absent. Repeated and long time irradiation of the sample show the high stability of the photoconduction phenomenon in the C_{60}@Zn(TPP) SURMOF (Figure S10). Noteworthy, the light irradiation increases the conduction of this sample by approximately four orders of magnitude.

To elucidate the mechanism of charge transport in C_{60}@Zn(TPP), a state of the art quantum chemical analysis has been carried out. To this end, we calculated the electronic coupling elements between the MOF linkers using a previ ously developed fully ab initio Quantum Patch method[22] based on molecular orbitals, estimated from density func tional theory (DFT). For these calculations, the C_{60}@Zn(TPP) structure, optimized using periodic approach, as described in the Supporting Information, was used. Typical for MOFs, as a result of the charge localization and large distance between the molecular units in the MOF, the electronic coupling elements in the crystalline framework are generally small.[23] We find that the electronic coupling of the Zn(TPP) HOMO orbitals (6.20 meV) is one order of magnitude larger than of other intermolecular pairs in the MOF (Table S2). This suggests that hole transport is provided within stacks of porphyrin linkers, which are localized along the *z* axis (Fig ure S13).

The electronic coupling of the porphyrin LUMO orbitals (0.27 meV) is approximately three times lower than for the LUMO orbitals in the Zn(TPP) C_{60} molecular pair (1 meV), see Table S2, indicating higher propensity for direct electron transfer (ET) between porphyrin and C_{60}.

Additionally, owing to the donor acceptor interactions in Zn(TPP) C_{60} and the strong electronegative character of C_{60} with the low energy levels (Figure 4), there is a high rate for

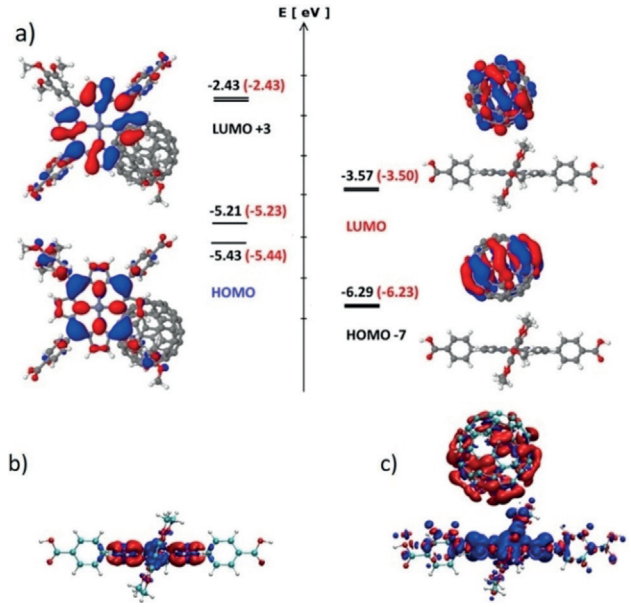

Figure 4. a) Visualized HOMO and LUMO orbitals of the Zn(TPP) linker (left) and C_{60} (right) with the corresponding orbital energies. While the energies of the Zn(TPP) C_{60} complex are shown in black, the energies of the isolated Zn(TPP) and C_{60} are red. The labeling of orbitals, that is, HOMO 7 and LUMO + 3, corresponds to orbitals in the Zn(TPP) C_{60} complex. b), c) Electron density difference upon the singlet singlet excitation of isolated porphyrin (b) and porphyrin in Zn(TPP) C_{60} complex (c). The electron accepting regions are labelled in red and electron donating regions are labelled in blue. The electron transition from TPP to C_{60} is clearly visible. Electronic properties were calculated using B3LYP functional with def2 SV(P) basis set and Grimme D3 dispersion correction using Turbomole[26] 7.1 (see Supporting Information).

light induced electron transfer to C_{60}, which permits carriers to move towards the respective electrode through the C_{60} channels. Here, the electronic coupling element of the LUMO orbitals is 0.33 meV, but is prone to increase significantly when the fullerene intermolecular distance decreases. As a result, the photo induced charge carriers in C_{60}@Zn(TPP) flow in separated domains: holes within porphyrin linkers and electrons within fullerene channels. A similar phenomenon was reported for hexa zirconium(IV) MOF loaded with C_{60}.[8] The same tendency was predicted theoretically[24] and confirmed experimentally[25] for porphyrin fullerene organic films.

Combination of Zn(TPP) SURMOF with C_{60} results in more efficient photoactivated ET and exciton separation. This is depicted in Figure 4 b,c, which shows the electron density difference after the porphyrin photoexcitation. The donor acceptor interface in C_{60}@Zn(TPP) (Figure S13) enables intermolecular charge separation (Figure 4 c), in which the recombination of the generated electron hole pair and the rate of electron back transfer decrease. This increases the number of mobile charge carriers after the photoexcitation in C_{60}@Zn(TPP). Therefore, the photoconductance of C_{60}@Zn (TPP) results from the combination and mutual orientation of both, electron donor porphyrin and electron acceptor C_{60}: The Soret band of the electron donor porphyrin is optically excited by blue (455 nm) light and the electron acceptor C_{60} significantly improves the photoactivated electron transfer from porphyrin as a result of the effective long range charge separation and the reduction of the charge recombination, as known for C_{60}.[27] The structure of C_{60}@Zn(TPP) with high density of donor acceptor interfaces, together with the spatially continuous network of interpenetrating donor and acceptor domains, provides a mechanism not only for exciton formation upon photoexcitation, but also an efficient charge separation and transport of the generated charge carriers through the MOF material, resulting in enhanced photo conduction properties of C_{60}@Zn(TPP).

Among the advantages of using combinations of functional molecules in the regular order of a MOF is that both active components, porphyrin and fullerene, can be modified without modifying the crystal structure. This is demonstrated by constructing a different SURMOF, C_{60} COOH@Zn(DAP) containing fullerene guests (C_{60} COOH), built from a different porphyrin linker (DAP = [10,20 bis(4 carboxyphenyl) 5,15 diazaporphyrinato]zinc(II), see Figure S14). For this different MOF thin film, the photoconductance properties are similar (Figure S18). The current increase upon blue light irradiation also amounts to about 2 orders of magnitude, however, the absolute current values in C_{60} COOH@Zn (DAP) are smaller than in C_{60}@Zn(TPP). Remarkably, as a result of the different electronic structures and absorption spectra of the DAP porphyrin, the photoconduction response to light of different wavelengths is slightly different. For example, while the ratio of the photocurrent during irradiation with 455 nm compared to irradiation with 400 nm is 2.2 for C_{60}@Zn(TPP), it is 2.6 in C_{60} COOH@Zn(DAP).

In comparison to other thin films possessing photoactive porphyrins, for example, films of porphyrin functionalized gold nanoparticles or porphyrin decorated graphene sheets,[28] the C_{60}@Zn(TPP) SURMOF has a significantly larger on off photocurrent ratio. The superior photoconduction properties of the SURMOF are presumably caused by the regular, crystalline order, allowing a high charge carrier mobility.[12] Similarly large photocurrent ratios as in C_{60}@Zn (TPP) were achieved with ordered molecular assemblies of various porphyrin derivatives in the form of crystalline nanorods and nanowires,[18a,29] however, the crystalline assembly of such materials in the form of thin films with controlled thickness has not yet been demonstrated. The crystalline assembly also allows for the precise structure determination, enabling a thorough theoretical analysis of the charge transport with a reliable identification of basic mechanisms. In addition, the oriented SURMOF structure results in efficient charge transfer in the direction of the closely packed C_{60} and porphyrin molecules, which are forming charge transfer

channels parallel to the surface, connecting the electrodes. These channels resemble ideal nanostructured donor acceptor hole and electron transporting highways for photo current generation.

In conclusion, crystalline, oriented MOF thin films with porphyrinic linkers and C_{60} embedded in the pores were prepared. Photoconduction behavior under irradiation with blue light, exciting the porphyrin Soret band, was found to increase the electrical conductivity of the SURMOFs by 2 orders of magnitude. The photoconductance is a result of both, the photosensitive porphyrin acting as the electron donor and the C_{60} acting as the electron acceptor, in addition to the designed MOF structure, which enables effective electronic coupling within the donor and acceptor phases. As a result of the efficient exciton separation and transport of the generated electron hole pairs within the spatially continuous network of donor and acceptor domains, hole and electron transport is provided through the close packed Zn(TPP) MOF linkers and C_{60} channels, respectively.

Based on the virtually unlimited possibilities to tune the properties by appropriate molecular functionalizations of C_{60} as an electron acceptor and porphyrin as an electron donor as well as to tune the absorption properties and absorption wavelength, the MOF photoconductivity properties can be varied and adopted.

Acknowledgements

L.X. acknowledges the financial support from Chinese Scholarship Council (CSC). M.K. is very grateful to F. Symalla and A. Fediai for fruitful discussions and S. Heidrich for the periodic calculations. We acknowledge funding by M ERA.NET MODIGLIANI and SFB 1176. This work was performed on the computational resource ForHLR II funded by the Ministry of Science, Research and the Arts Baden Württemberg and DFG ("Deutsche Forschungsgemein schaft"). C.W. and S.M. thank financial support by the DFG through SPP COORNET. This work was also supported by the JSPS (KAKENHI Grant Numbers JP18K14198 (T.H.) and JP18H03898 (H.I.)). L.H. acknowledges funding by the Volkswagen foundation and the DFG (HE7036/5). We thank Frank Kirschhöfer and Michael Nusser (IFG, KIT) for the help with the mass spectrometry.

Conflict of interest

The authors declare no conflict of interest.

Keywords: C_{60} fullerene · density functional theory · metal organic frameworks (MOFs) · photoconduction · porphyrin

[1] a) S. Kaskel, *The Chemistry of Metal Organic Frameworks: Synthesis Characterization, and Applications*, Wiley, Hoboken, **2016**; b) H. Furukawa, K. E. Cordova, M. O'Keeffe, O. M. Yaghi, *Science* **2013**, *341*, 1230444.

[2] a) B. Seoane, J. Coronas, I. Gascon, M. Etxeberria Benavides, O. Karvan, J. Caro, F. Kapteijn, J. Gascon, *Chem. Soc. Rev.* **2015**, *44*, 2421 2454; b) H. W. Langmi, J. W. Ren, B. North, M. Mathe, D. Bessarabov, *Electrochim. Acta* **2014**, *128*, 368 392.

[3] a) C. G. Silva, A. Corma, H. Garcia, *J. Mater. Chem.* **2010**, *20*, 3141 3156; b) A. A. Talin, A. Centrone, A. C. Ford, M. E. Foster, V. Stavila, P. Haney, R. A. Kinney, V. Szalai, F. El Gabaly, H. P. Yoon, F. Leonard, M. D. Allendorf, *Science* **2014**, *343*, 66 69; c) A. Dragässer, O. Shekhah, O. Zybaylo, C. Shen, M. Buck, C. Wöll, D. Schlettwein, *Chem. Commun.* **2012**, *48*, 663 665; d) L. M. Montañez, K. Müller, L. Heinke, H. J. Osten, *Micro porous Mesoporous Mater.* **2018**, *265* 185 188.

[4] P. Z. Moghadam, A. Li, S. B. Wiggin, A. Tao, A. G. P. Maloney, P. A. Wood, S. C. Ward, D. Fairen Jimenez, *Chem. Mater.* **2017**, *29*, 2618 2625.

[5] A. Morozan, F. Jaouen, *Energy Environ. Sci.* **2012**, *5*, 9269 9290.

[6] G. D. Wu, J. H. Huang, Y. Zang, J. He, G. Xu, *J. Am. Chem. Soc.* **2017**, *139*, 1360 1363.

[7] D. Sheberla, J. C. Bachman, J. S. Elias, C. J. Sun, Y. Shao Horn, M. Dinca, *Nat. Mater.* **2017**, *16*, 220 224.

[8] S. Goswami, D. Ray, K. i. Otake, C. W. Kung, S. J. Garibay, T. Islamoglu, A. Atilgan, Y. Cui, C. J. Cramer, O. K. Farha, *Chem. Sci.* **2018**, *9*, 4477 4482.

[9] M. R. Pederson, A. A. Quong, *Phys. Rev. B* **1992**, *46*, 13584 13591.

[10] G. Yu, J. Gao, J. C. Hummelen, F. Wudl, A. J. Heeger, *Science* **1995**, *270*, 1789 1791.

[11] S. Hamel, V. Timoshevskii, M. Cote, *Phys. Rev. Lett.* **2005**, *95*, 146403.

[12] J. Liu, W. Zhou, J. Liu, I. Howard, G. Kilibarda, S. Schlabach, D. Coupry, M. Addicoat, S. Yoneda, Y. Tsutsui, T. Sakurai, S. Seki, Z. Wang, P. Lindemann, E. Redel, T. Heine, C. Wöll, *Angew. Chem. Int. Ed.* **2015**, *54*, 7441 7445; *Angew. Chem.* **2015**, *127*, 7549 7553.

[13] A. Dhakshinamoorthy, A. M. Asiri, H. Garcia, *Angew. Chem. Int. Ed.* **2016**, *55*, 5414 5445; *Angew. Chem.* **2016**, *128*, 5504 5535.

[14] A. Takai, C. P. Gros, J. M. Barbe, R. Guilard, S. Fukuzumi, *Chem. Eur. J.* **2009**, *15*, 3110 3122.

[15] L. L. Li, E. W. G. Diau, *Chem. Soc. Rev.* **2013**, *42*, 291 304.

[16] a) H. Imahori, T. Umeyama, S. Ito, *Acc. Chem. Res.* **2009**, *42*, 1809 1818; b) A. D. Schwab, D. E. Smith, B. Bond Watts, D. E. Johnston, J. Hone, A. T. Johnson, J. C. de Paula, W. F. Smith, *Nano Lett.* **2004**, *4*, 1261 1265; c) M. Muccini, *Nat. Mater.* **2006**, *5*, 605 613.

[17] a) H. Imahori, *Bull. Chem. Soc. Jpn.* **2007**, *80*, 621 636; b) D. Kuciauskas, S. Lin, G. R. Seely, A. L. Moore, T. A. Moore, D. Gust, T. Drovetskaya, C. A. Reed, P. D. W. Boyd, *J. Phys. Chem.* **1996**, *100*, 15926 15932; c) M. E. El Khouly, C. A. Wijesinghe, V. N. Nesterov, M. E. Zandler, S. Fukuzumi, F. D'Souza, *Chem. Eur. J.* **2012**, *18*, 13844 13853; d) F. D'Souza, G. R. Deviprasad, M. E. Zandler, M. E. El Khouly, M. Fujitsuka, O. Ito, *J. Phys. Chem. B* **2002**, *106*, 4952 4962; e) E. Krokos, F. Spaenig, M. Ruppert, A. Hirsch, D. M. Guldi, *Chem. Eur. J.* **2012**, *18*, 1328 1341.

[18] a) R. Charvet, Y. Yamamoto, T. Sasaki, J. Kim, K. Kato, M. Takata, A. Saeki, S. Seki, T. Aida, *J. Am. Chem. Soc.* **2012**, *134*, 2524 2527; b) T. Hasobe, S. Fukuzumi, P. Kamat, *Electrochem. Soc. Interface* **2006**, *15*, 47 51; c) C. Y. Lee, J. K. Jang, C. H. Kim, J. Jung, B. K. Park, J. Park, W. Choi, Y. K. Han, T. Joo, J. T. Park, *Chem. Eur. J.* **2010**, *16*, 5586 5599; d) K. Sakakibara, F. Nakatsubo, *Macromol. Chem. Phys.* **2008**, *209*, 1274 1281; e) T. Hasobe, H. Imahori, S. Fukuzumi, P. V. Kamat, *J. Phys. Chem. B* **2003**, *107*, 12105 12112; f) A. Kira, T. Umeyama, Y. Matano, K. Yoshida, S. Isoda, J. K. Park, D. Kim, H. Imahori, *J. Am. Chem.*

Soc. **2009**, *131*, 3198 3200; g) H. Nobukuni, F. Tani, Y. Shimazaki, Y. Naruta, K. Ohkubo, T. Nakanishi, T. Kojima, S. Fukuzumi, S. Seki, *J. Phys. Chem. C* **2009**, *113*, 19694 19699; h) T. Hasobe, *J. Phys. Chem. Lett.* **2013**, *4*, 1771 1780.

[19] S. Wang, T. Kitao, N. Guillou, M. Wahiduzzaman, C. Martineau Corcos, F. Nouar, A. Tissot, L. Binet, N. Ramsahye, S. Devautour Vinot, S. Kitagawa, S. Seki, Y. Tsutsui, V. Briois, N. Steunou, G. Maurin, T. Uemura, C. Serre, *Nat. Commun.* **2018**, *9*, 1660.

[20] a) J. X. Liu, C. Wöll, *Chem. Soc. Rev.* **2017**, *46*, 5730 5770; b) O. Shekhah, H. Wang, S. Kowarik, F. Schreiber, M. Paulus, M. Tolan, C. Sternemann, F. Evers, D. Zacher, R. A. Fischer, C. Wöll, *J. Am. Chem. Soc.* **2007**, *129*, 15118 15119; c) L. Heinke, C. Wöll, *Adv. Mater.* **2019**, 1806324 https://doi.org/10.1002/adma.201806324.

[21] a) W. Guo, Z. Chen, C. Yang, T. Neumann, C. Kuebel, W. Wenzel, A. Welle, W. Pfleging, O. Shekhah, C. Wöll, E. Redel, *Nanoscale* **2016**, *8*, 6468 6472; b) L. Heinke, C. Wöll, *Phys. Chem. Chem. Phys.* **2013**, *15*, 9295 9299.

[22] a) P. Friederich, F. Symalla, V. Meded, T. Neumann, W. Wenzel, *J. Chem. Theory Comput.* **2014**, *10*, 3720 3725; b) P. Friederich, V. Meded, F. Symalla, M. Elstner, W. Wenzel, *J. Chem. Theory Comput.* **2015**, *11*, 560 567; c) P. Friederich, V. Meded, A. Poschlad, T. Neumann, V. Rodin, V. Stehr, F. Symalla, D. Danilov, G. Luedemann, R. F. Fink, I. Kondov, F. von Wrochem, W. Wenzel, *Adv. Funct. Mater.* **2016**, *26*, 5757 5763.

[23] a) T. Neumann, J. Liu, T. Waechter, P. Friederich, F. Symalla, A. Welle, V. Mugnaini, V. Meded, M. Zharnikov, C. Wöll, W. Wenzel, *ACS Nano* **2016**, *10*, 7085 7093; b) S. Garg, H. Schwartz, M. Kozlowska, A. B. Kanj, K. Müller, W. Wenzel, U. Ruschewitz, L. Heinke, *Angew. Chem. Int. Ed.* **2019**, *58*, 1193 1197; *Angew. Chem.* **2019**, *131*, 1205 1210.

[24] A. Buldum, D. H. Reneker, *Nanotechnology* **2014**, *25* 235201.

[25] A. S. Konev, A. F. Khlebnikov, O. V. Levin, D. A. Lukyanov, I. M. Zorin, *ChemSusChem* **2016**, *9*, 676 686.

[26] R. Ahlrichs, M. Bär, M. Häser, H. Horn, C. Kölmel, *Chem. Phys. Lett.* **1989**, *162*, 165 169.

[27] a) H. Imahori, Y. Sakata, *Adv. Mater.* **1997**, *9*, 537 546; b) D. M. Guldi, C. Luo, M. Prato, E. Dietel, A. Hirsch, *Chem. Commun.* **2000**, 373 374.

[28] a) M. Miyachi, Y. Yamanoi, K. Nakazato, H. Nishihara, *Biochim. Biophys. Acta Bioenerg.* **2014**, *1837*, 1567 1571; b) Y. Hu, Z. Xue, H. He, R. Ai, X. Liu, X. Lu, *Biosens. Bioelectron.* **2013**, *47*, 45 49; c) M. S. Choi, D. J. Lee, S. J. Lee, D. H. Hwang, J. H. Lee, N. Aoki, Y. Ochiai, H. J. Kim, D. Whang, S. Kim, S. W. Hwang, *Appl. Phys. Lett.* **2012**, *100*, 163116.

[29] a) H. Mai Ha, Y. Kim, M. Kim, K. H. Kim, T. W. Lee, N. Duc Nghia, S. J. Kim, K. Lee, S. J. Lee, D. H. Choi, *Adv. Mater.* **2012**, *24*, 5363 5367; b) F. X. Wang, J. Lin, Y. Q. Liu, H. D. Wu, G. B. Pan, *Org. Electron.* **2014**, *15*, 844 849; c) H. X. Ji, J. S. Hu, L. J. Wan, *Chem. Commun.* **2008**, 2653 2655.

[30] K. Müller, J. Helfferich, F. L. Zhao, R. Verma, A. B. Kanj, V. Meded, D. Bléger, W. Wenzel, L. Heinke, *Adv. Mater.* **2018**, *30*, 1706551.